Brain transcriptomics reveals features of the host response after dengue virus type I infection induced central nervous system injury in AGB6 mice

Ning Yu [a, b], Shigang Chen [a, b], Yumeng Liu [b, c], Peng Wang [b, d], Longlong Wang [b], Ningning Hu [b], He Zhang [b], Xiao Li [b,e], Huijun Lu [b, d,e]*, Ningyi Jin [a, b, c, d, e]*

[a] College of Veterinary Medicine, Jilin University, Changchun, People's Republic of China; [b] Laboratory of Molecular Virology and Immunology, Changchun Veterinary Research Institute, Chinese Academy of Agricultural Sciences, Changchun, People's Republic of China; [c] Animal Science and Technology College, Guangxi University, Guangxi, People's Republic of China; [d] College of Animal Sciences Zhejiang University, Hangzhou, People's Republic of China; [e] Research Unit of Key Technologies for Prevention and Control of Virus Zoonoses, Chinese Academy of Medical Sciences, Changchun, People's Republic of China.

*huijun_lu@126.com (Huijun Lu); ningyik@126.com (Ningyi Jin)

ABSTRACT

Dengue viruses are the causative agents of dengue fever, dengue hemorrhagic fever, and dengue shock syndrome, which are mainly transmitted by Aedes aegypti and Aedes albopictus mosquitoes, and cost billions of dollars annually in medical and mosquito control. It is estimated that up to 20% of dengue virus infections affect the brain. The incidence of DENV infection of the nervous system is increasing, suggesting that more people are at risk for neurological complications of the infection. Currently, understanding the pathogenic mechanisms of dengue virus infection of the nervous system is hampered by the lack of suitable small animal models. Here, we analyzed the pathogenicity of dengue virus in type I and type II interferon receptor-deficient mice by intraperitoneal inoculation of DENV-I. Infected mice showed such neurological symptoms as opisthotonus, hunching, ataxia, and paralysis of one or both hind limbs. Viremia can be detected 3 days after infection. The virus showed evident brain tropism post-inoculation and viral loads peaked at 14 days post-inoculation in infected mice brain. Significant histopathologic changes were observed in brain tissue (hippocampal region and cerebral cortex). Immunohistochemistry and fluorescence showed clear

fluorescent signals. Hematological analysis showed hemorrhage and hemoconcentration in DENV-I infected mice. Subsequently, brain tissue transcriptome sequencing was performed to assess host response characteristics in DENV-I infected AGB6 mice. Functional enrichment analysis and analysis of significantly differentially expressed genes (DEGs) were used to identify the key molecular mechanisms of brain tissue injury. Transcriptional patterns in brain tissue suggest that aberrant expression of pro-inflammatory cytokines induces antiviral responses to dengue virus and tissue damage. Combined with the KEGG results, it was hypothesized that the probable cause of the neurological damage affecting the neurological system and hindlimb paralysis was the marked enrichment of upregulated DEGs in the cytokine-cytokine receptor interaction signaling pathway. Screening of hub genes and their characterization by qPCR and ELISA, it was hypothesized that IL-6 and IFN-γ might be the key factors in dengue virus-induced neurological manifestations.

KEYWORDS Dengue virus; AGB6 mice; CNS injury; transcriptomics

Introduction

Dengue virus belongs to the *Flaviviridae* family, *Flavivirus* genus, a single-stranded positive-stranded RNA virus, which is a mosquito-borne virus like West Nile virus, Zika virus, and yellow fever virus[1]. The genome of this virus has only one open reading frame (ORF), which is translated into a multimeric protein, which is subsequently broken down into three structural and seven nonstructural proteins catalyzed by host proteases and the virus's protease, and performs their respective functions. The order of the encoded proteins is 5'-C-PrM-E-NS1-NS2a-NS2b-NS3-NS4a-NS4b-NS5-3'[2, 3]. According to their surface antigenicity, dengue viruses are classified into four serotypes DENV-I, DENV-II, DENV-III, and DENV-IV[4]. DENV-I was first detected in 1943 in French Polynesia and Japan and seemed to be the most reported serotype between 1943 and 2013[5, 6]. Dengue fever is a self-limiting disease; most people with dengue have no or mild symptoms, and severe cases can cause dengue hemorrhagic fever (DHF) and dengue shock syndrome (DSS) [7, 8]. Dengue fever is expected to infect an estimated 100 million to 400 million people each year[9], posing a significant threat to the global economy and health.

Dengue viruses were earlier misidentified as non-neurophilic, and in 2009, the WHO released new guidelines and classifications for dengue, which included CNS

69   involvement in the definition of severe disease[10]. Manifestations of meningitis,
70   encephalitis, Guillain-Barre syndrome (GBS), acute demyelinating encephalopathy
71   (ADEM), myelitis, polyneuropathy, and mononeuropathy[11]. The incidence of
72   encephalopathy and encephalitis, the most common neurological complications of
73   dengue, has been estimated to be between 0.5 and 6.2%[12]. Currently, the pathogenesis
74   of dengue neurologic disorders is incompletely understood. Three mechanisms may be
75   operative: direct CNS invasion by the virus, autoimmune reactions, and metabolic
76   alterations[13].

77   Transcriptome sequencing enables the study of gene function and gene structure
78   at a holistic level, revealing the molecular mechanisms involved in specific biological
79   processes as well as in the development of diseases. Clinical data have demonstrated a
80   significant relationship between brain tissue damage and severe dengue fever[14-16].
81   Currently, there is no breakthrough in the study of the pathogenic mechanism of dengue
82   virus-induced encephalitis, and there is still a need to explore the general features of
83   host inflammatory and immune responses in DENV-infected mouse models, especially
84   the transcriptional responses in brain injury, which may reveal potential therapeutic
85   targets from a holistic perspective.

86   In this study, we aimed to assess the transcriptomic profile of brain tissue in a
87   mouse model of dengue virus infection based on a lethal animal model, followed by a
88   series of functional analyses to partially elucidate the underlying pathogenesis of
89   dengue virus-induced brain damage.

90

Materials and methods

Cell culture

93   The African green monkey kidney cells (Vero) were cultured in DMEM medium
94   supplemented with 10% FBS. An *Aedes albopictus* gut line (C6/36) was purchased
95   from the National Collection of Authenticated Cell Cultures. C6/36 cells were cultured
96   in MEM medium with 15% fetal bovine serum (FBS) and incubated in a humidified
97   atmosphere containing 5% CO_2 at 28°C.

98

Virus strain

100   The virus strain used in the study derives from a patient in RuiLi, YunNan Province
101 in 2017 that has been exclusively passaged for about 6 rounds in C6/36 cells (GenBank
102 number: OM250394). For AGB6 infection, viruses were harvested and concentrated

using a 10K MWCO Amicon (Merck) at 1500×g, 4°C, for 2 hours, then quantified by immunoperoxidase monolayer assays in Vero cells. Virus titer after concentration was $10^{5.63}/0.1$ mL.

Mice

Male AGB6 mice (deficient in both type I and type II interferon receptor) were a cross between *Ifnar^{-/-}* mice (C57BL/6 background) and *Ifngr^{-/-}* mice (C57BL/6 background) were purchased from Shanghai Model Organisms Center, Inc. Female C57BL/6 and BALB/c were purchased from Beijing Viton Lihua Laboratory Animal Technology Co. They were housed in the Animal Biological Safety Level-2 laboratory (ABSL-2) at Changchun Veterinary Research Institute and were provided access to food and water. Unless otherwise specified, both male and female mice between the ages of 5-6 weeks were used in the study.

Mice infection

To test the virulence of the DENV-I, twenty-five AGB6 mice were randomly divided to five groups. They were administered with 10^8 to 10^5 TCID$_{50}$ of DENV-I via the intraperitoneal (IP.) route (0.5 mL in sterile PBS). Mice injected with an equivalent volume of PBS (mock infection) were used as the negative control. Animals were monitored for clinical phenotypes, morbidity, and mortality. For the 10^7 TCID$_{50}$ infected group. At 3, 7, and 11 dpi (n=3), blood was taken from the tail vein to determine viremia, then mice were euthanized with tribromoethanol, and the tissues (heart, liver, spleen, lung, kidney, brain, jejunum, ileum, caecum, colon, rectum) were quickly homogenized on ice and stored at -40°C for further use. When a humane endpoint (body weight loss of ≥20%, hunched posture, ruffled fur, conjunctivitis, movement impairment, lower limb paralysis) was reached, mice (n=3) were euthanized, the half of brain was collected and quick-frozen in liquid nitrogen, and then RNA was extracted for transcriptome sequencing.

To clarify the infection of DENV-I in immunocompetent mice. C57BL/6 (n=12) and BALB/c (n=12) mice were administered with 10^7 TCID$_{50}$ of DENV-I via the intraperitoneal (IP.) route (0.5 mL of sterile PBS). They were weighed and the course of the disease was monitored until 15 dpi. Blood and tissues (n=3) were collected at the same intervals selected for the infected group of AGB6 mice (10^7 TCID$_{50}$) and stored at -40 for subsequent analysis.

137

Quantitative real-time (qRT) PCR

The total RNA was extracted from the blood, heart, liver, spleen, lung, kidney, brain, jejunum, ileum, caecum, colon, and rectum (obtained from AGB6 mice, C57BL/6 mice and BALB/c mice) using a Total RNA Extractor kit (Sangon Biotech, China). Using the HiScript II U+ One Step qRT-PCR Probe Kit (Vazyme, Nanjing), 150 µg of RNA was pipetted for amplification. Using previously established assays, serial dilutions of the pUC57-DENV plasmid with known concentrations were used to establish the standard curve. RNA copies per mL or RNA copies per gram of each sample were calculated from the Ct values.

The M-MLV Reverse Transcriptase Kit was used to reverse-transcribe the total RNA to cDNA. The relative expression levels of IL-1β, IL-6, IFN-γ, TNFα, CCL2, CCL3, CCL4, and CCL5 were determined using RT-PCR. Mouse GAPDH internal reference primers were purchased from Sangon Biotech (Shanghai) Co., Ltd. The primers used in this study are listed in Supplementary Table S1.

152

Viral protein detection

For Western blot analysis, 10 µL of tissue slurry samples were run on a 10%-15% Bis-Tris SDS-PAGE gel as described previously[17]. The Nitrocellulose (NC) membranes were incubated with Anti-DENV-E gene (Abcam, ab9202) and NS1 gene (Genetex, GTX124280) antibodies. Horseradish peroxidase (HRP) secondary antibody (Beyotime, A0216) was used at a 1:2000 dilution. NC membranes were imaged on an Amersham Imager 600 (General Electric, USA).

160

Antibody titers

Systemic antibody titers against DENV-I were determined by Enzyme-linked Immunosorbent Assays (ELISA) as described previously[18]. Briefly, 96-well plates were coated overnight at 4°C with 10^5 TCID$_{50}$/0.1mL of heat-inactivated DENV-I in 0.1M NaHCO$_3$ buffer at pH 9.6. Two-fold serially diluted serum samples (1:50 to 1:102,400) were added to the wells and incubated for 2 hours at 37°C. HRP-conjugated anti-mouse IgM (Abcam, ab97230) and IgG (H+L) (Abcam, ab6808) secondary antibodies were used. The ELISA titers were defined as the reciprocal of the highest serum dilution that equals to 3 times the absorbance reading from uninfected mouse serum sample.

171

Histopathology Staining

Paraffin-embedded tissue sections (slice thickness of 4μm) were dewaxed with xylol, hydrated with ethanol, and stained with hematoxylin for 5 min and eosin for 3 min. Images were photographed using a 20× objective with the Eclipse C1 microscope (Nikon, Tokyo, Japan) equipped with a DS-U3 camera (Nikon, Tokyo, Japan).

Immunofluorescence Staining

For cells, after four days of infection, the plate was fixed for 30 min with 4% paraformaldehyde (PFA). The cells were permeabilized with 0.5% TritonX-100 for 15 min. Infected cells were detected with monoclonal anti-dengue-NS3 antibody (Genetex, GTX124252) and FITC-conjugated secondary antibody (Beyotime, A0568). Finally, the cells were stained with Hoechst (Thermo Fisher Scientific, 62249) for 10 minutes and images were photographed with EVOS M5000 imaging system (Thermo Fisher Scientific, USA).

For mouse tissues, immunofluorescence staining was carried out as described previously[19]. Briefly, sections were repaired using EDTA antigen recovery buffer and incubated overnight at 4 °C with anti-dengue virus 1+2+3+4 primary antibody (Abcam, ab26837). Next, sections were incubated with CY3-conjugated secondary antibodies for 50 min and 4,6-diamidino-2-phenylindole (DAPI) for 10 min. Images were photographed using a 20× objective with the Eclipse C1 microscope (Nikon, Tokyo, Japan) equipped with a DS-U3 camera (Nikon, Tokyo, Japan).

Transmission Electron Microscopy

The brain tissues were quickly fixed with 2.5% glutaraldehyde overnight at 4 °C. After rinsing with PBS and fixation with 1% osmotic acid for 2 hours. Following graded acetone dehydration, tissues were infiltrated, embedded and polymerized in resin. The sections (70 nm) were stained with 2% uranyl acetate-saturated aqueous solution and lead citrate for 15 min. Imaged using a TECNAI G2 20 TWIN TEM transmission electron microscope (FEI, USA).

Hematology

Blood (100 μl) was collected in 1 ml EDTA-K2 tubes to prevent clotting and was then briefly vortexed, and whole blood analysis was carried out using an automatic

205 animal blood cell analyzer (TEK-VET3, China). The hematology parameters analysis
206 included the lymphocytes, neutral counts, red and white blood cell counts, hematocrit,
207 and platelet count.
208

209 ***Cytokine detection***

210   Expression levels of cytokines (IL-1β, IL-6, IFN-γ, TNF-α) were assayed in mouse
211 brain tissue grindings according to the manufacturer's instructions using different assay
212 kits (Cloud-Clone Corp, China).
213

214 ***RNA library preparation and sequencing***

215   Total RNA was extracted from mouse brain tissue using total RNA Extractor
216 (Trizol) according to the manufacturer's protocol (Sangon Biotech, Shanghai). Total
217 amounts and integrity of RNA were assessed using the RNA Nano 6000 Assay Kit of
218 the Bioanalyzer 2100 system (Agilent Technologies, CA, USA). Then, libraries were
219 constructed using a TruSeq Stranded mRNA LT Sample Prep Kit (Illumina, San Diego,
220 CA, USA) according to the manufacturer's instructions.

221   Libraries were sequenced on the Illumina NovaSeq 6000 platform, and 150 bp
222 paired-end reads were generated. Index of the reference genome was built using Hisat2
223 (v2.0.5)[20]. The fragments per kb of transcript per million mapped reads (FPKM) was
224 calculated using Feature Counts (v1.5.0-p3)[21].
225

226 ***Identification of differentially expressed genes and functional enrichment***

227   Using the DESeq2 R package (1.20.0), differential expression analysis of two
228 groups (three biological replicates) was carried out. The P values were adjusted using
229 the Benjamini & Hochberg method. For considerably differential expression, p-
230 adj<=0.05 and |log2(foldchange)| >= 1 were chosen as the cutoff values. GO and KEGG
231 enrichment analysis of differentially expressed genes by Clusterprofiler (3.8.1)
232 software.
233

234 ***Ethics statements and facility***

235   All procedures involving mice and experimental protocols of our study were
236 approved by the Animal Ethics Committee of Changchun Veterinary Research Institute.
237 All animals were handled by the Animal Ethics Procedures and Guidelines of the
238 People's Republic of China, the principles described by the Animal Welfare Act, and

239 the National Institutes of Health Guidelines for the care and use of laboratory animals

240 in biomedical research. All animal experiments involving the dengue virus were

241 performed in the Animal Biological Safety Level-2 laboratory (ABSL-2) of Changchun

242 Veterinary Research Institute.

243

244 *Statistical analysis*

245 Data are expressed as the mean ± SD values. Comparison between experimental

246 and control groups was performed using an ordinary one-way ANOVA. Differences

247 with a probability value of $p<0.05$ were defined as significant. GraphPad Prism

248 (https://www.graphpad-prism.cn/) was used for statistical analyses and visualization.

249 Screening   for   dengue   virus-related   genes   using   DisGeNET

250 (https://www.disgenet.org)and Genecard (https://www.genecards.org) databases.

251

252 **Results**

253 *AGB6 mice can be efficiently infected by DENV-I via intraperitoneal inoculation*

254 To test the virulence of the DENV-I, AGB6 mice were intraperitoneally (ip.)

255 infected with 10-fold serially diluted viral doses ranging from 10^8 to 10^5 TCID$_{50}$.

256 Observe and record the survival rate, clinical symptoms, and weight changes of mice

257 for 15 consecutive days (Figure 1). Survival rates indicated that 10^7 TCID$_{50}$ and higher

258 dose induced 100% mortality, whereas 80% and 100% survival rates were observed in

259 animals infected with 10^6 and 10^5 TCID$_{50}$, respectively (Figure 1A). By measuring the

260 weight of mice, we found that mice infected with 10^8 TCID$_{50}$ experienced a rapid

261 decrease in weight on the 2 days post-infection (dpi), ultimately leading to mouse death

262 at 6dpi (Figure 1B); The mice infected with 10^7 TCID$_{50}$ showed fur wrinkles,

263 hunchback, lethargy, Ataxia and paralysis of one or both hind limbs between 10 and 14

264 dpi (Figure. 1C). It is worth noting that on the 4 dpi, the trend of weight loss of mice in

265 the 10^7 TCID$_{50}$ group was no different from that of mice in the 10^8 TCID$_{50}$ group.

266 However, on the 7 dpi, the weight of mice in the 10^7 TCID$_{50}$ group slowly increased,

267 and the status gradually recovered, until the rate of weight changes significantly

268 decreased after the onset of paralysis symptoms, ultimately leading to death (Figure

269 1B). The median lethal dose (LD$_{50}$) for DENV-I was $10^{6.6}$/0.5 mL, calculated by the

270 Reed-Muench method. The dose of virus infection is positively correlated with the time

271 of death, and heterogeneity increases with the decrease of infection dose.

272 Therefore, for experimental convenience and maximum stringency, a challenge

273   dose of 2.5 LD_{50} was used in subsequent studies and monitored the virus titer in the

274   blood during infection. The blood was collected at 3, 7, 11, and 14 dpi to detect the viral

275   load. At 3 dpi, viremia was detected by RT-PCR, with peak loads at around 7.16×10^5

276   copies/mL, followed by viral clearance from the blood circulation prior to animal death,

277   similar to the disease kinetic described in severe dengue fever (DF) patients (Figure

278   1D). Furthermore, specific IgG and IgM antibodies were detected during the course of

279   the infection, and significant IgG antibody titers were detected, which increased

280   gradually over time, peaking at 1:51200, while the IgM antibody response peaked at 7

281   dpi (1:12800) and waned by 11 dpi (Supplementary Figure S1 A, B).

282   In addition, neither disease manifestation nor transient viremia was observed in

283   immunocompetent BALB/c and C57BL/6 mice infected with 10^7 $TCID_{50}$ of DENV-I

284   by intraperitoneal injection (IP.). (Supplementary figure S2).
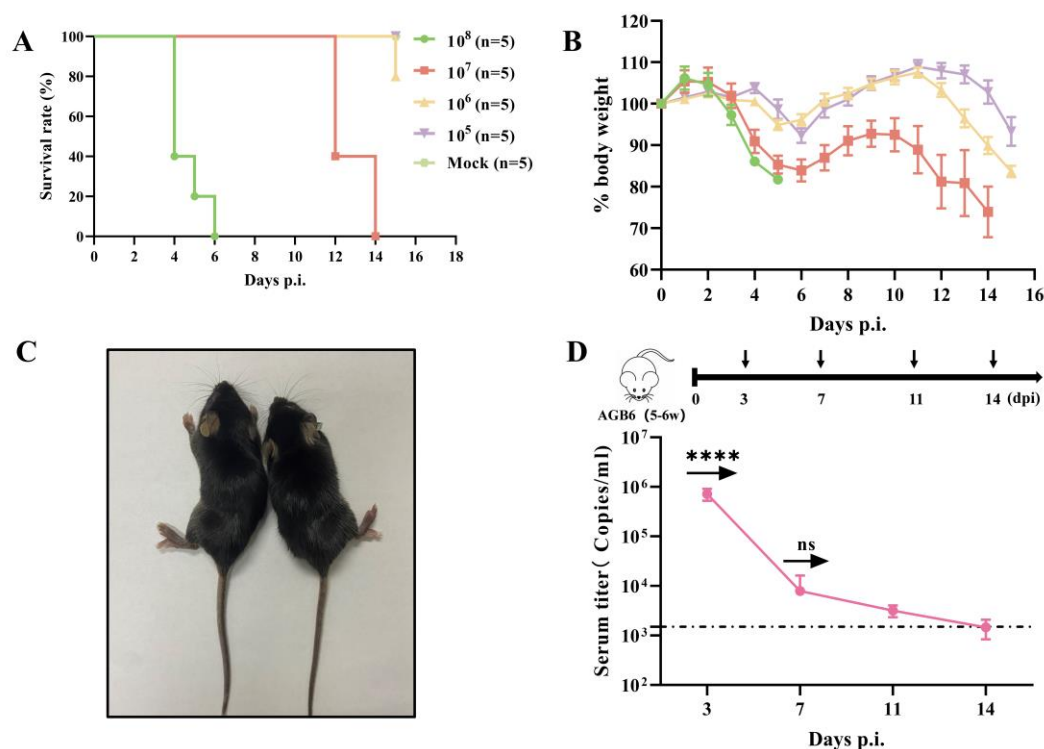

285

286   **Figure 1.** DENV-I lethal infection in AGB6 mice. **(A)** Survival probability of DENV-I

287   challenged AGB6 mice infection via IP. routes with different titers of DENV-I. **(B)**

288   Body weight was monitored daily. Results are expressed as the [mean ± SD] of body

289   weight loss in percentage compared to initial body weight. **(C)** Representative images

290   of paralysis symptoms in mice. Mice develop unilateral or bilateral hindlimb paralysis

291   at 12dpi. **(D)** Experimental scheme. 5-6 weeks old AGB6 mice were infected with 2.5

292   LD_{50} of DENV-I by IP. The blood of the challenged mice was harvested (black arrow).

293   The viremia was evaluated (n=3). The dotted black line indicates the limits of detection.

294   Abbreviations: IP., intraperitoneally. Ordinary one-way ANOVA test. ****, $p < 0.0001$;

295   ns, no significance.

296

297   ***DENV-I mainly infected brain in AGB6 mice***

298   In the previous study, we collected organs from AGB6 mice infected with DENV-

299   I virus to evaluate viral RNA, protein expression and histopathological changes

300   (Supplementary Figure S3). The viral protein NS1 was detected mainly in DENV-I

301   infected mice liver at 3 dpi. After 7 dpi, the viral protein E could be detected in brain,

302   with the highest expression during the moribund. In addition, different degrees of

303   pathologic changes were observed in the brain, spleen, lungs and liver, and no

304   significant pathologic changes were observed in other organs (Supplementary Figure

305   S4).

306   Most importantly, it was found that DENV RNA expression was highest in brain

307   tissue at moribund states (14 dpi). Therefore, the brain tissues were subjected to H&E

308   staining and histopathological observation, which revealed progressive damage at both

309   tissue and cellular levels which culminated at moribund states (Figure 2). As shown in

310   Figure 2A, In the hippocampus of DENV-I infected mice, degeneration of neuronal

311   cells in the granular layer (black arrows), infiltration of lymphocytes, monocytes and

312   neutrophils (red arrows), and swelling of the vascular endothelium (yellow arrows).

313   Cerebral cortical areas were the most severe, with neuronal cell necrosis (black arrows),

314   perivascular inflammatory cell infiltration (red arrows), and vasodilatation (blue

315   arrows). DENV-I infected cells were identified in neurons after staining with anti-NS3

316   antibody (Figure 2B). In addition, immunofluorescence staining showed clear

317   fluorescent signals in the brains of mice at moribund states (Figure 2C). Electron

318   microscopy analysis confirmed the presence of DENV-I particles in the brain of mice

319   at moribund states (red arrows) (Figure 2D).
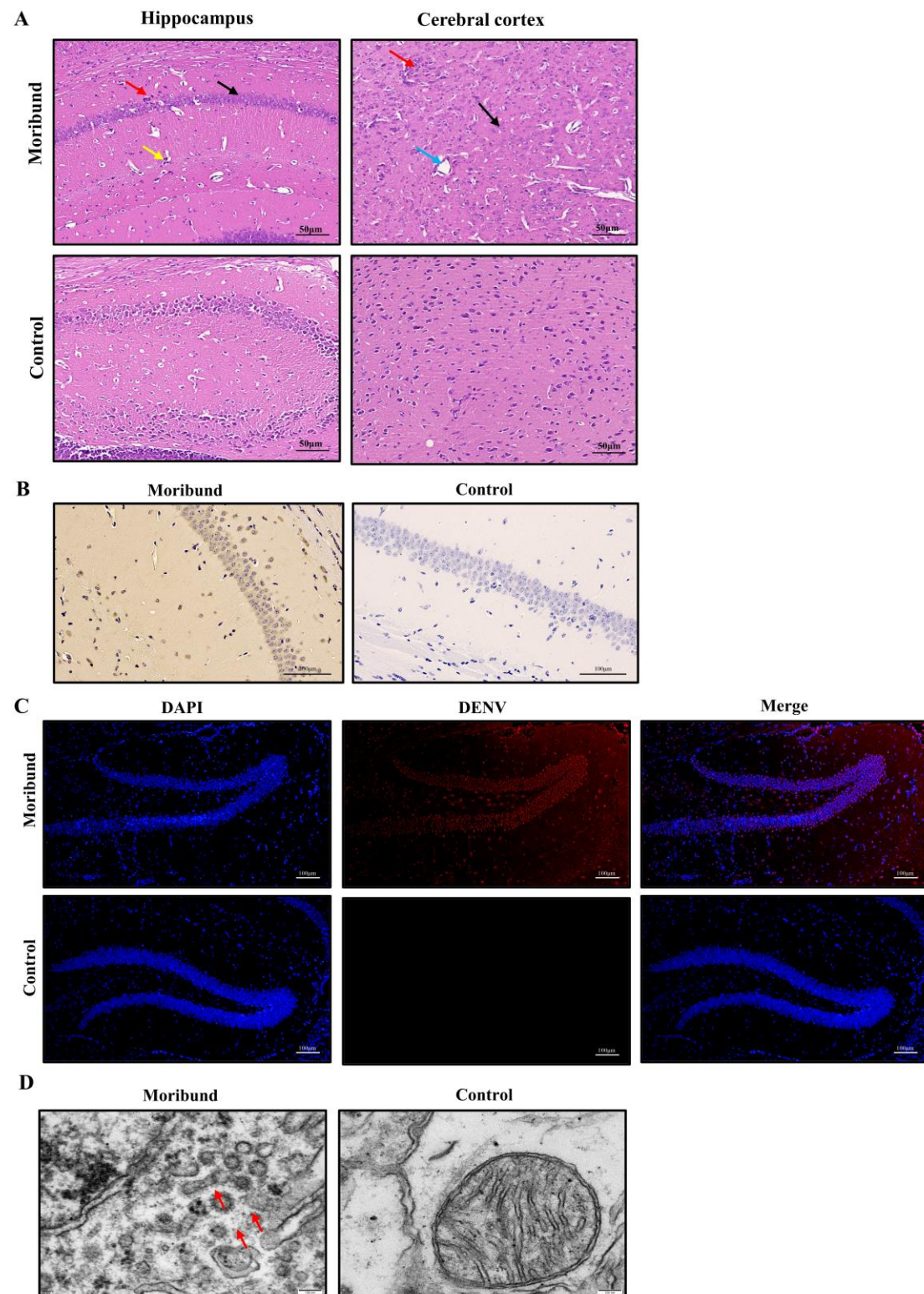
320

Figure 2. Infection status of brain tissue in DENV-I infected AGB6 mice. **(A)** Brains were harvested from IP. infected mice, and stained with H&E. Animals were euthanized at moribund states. Scale bar:50 μm. **(B)** Immunohistochemical staining of tissue sections from the DENV-I infected mice with an anti-NS3 antibody. **(C)**

325   Immunostaining of the hippocampal at moribund states. Sections were viewed under a

326   fluorescence microscope at 100 ×. Scale bar:100 μm. **(D)** Representative transmission

327   electron micrographs showing viral particles in DENV-I infected mouse brain.

328

329   ***Hematology in DENV-I infected AGB6 mice***

330   Hematology has been shown to be associated with dengue-associated diseases and

331   is tentatively used as a diagnostic and prognostic marker. To determine the effect of the

332   dengue virus on blood chemistry in AGB6 mice, blood was collected and analyzed on

333   3, 7, 11, and 14 dpi. The assays included white blood cells (WBC), red blood cells

334   (RBC), neutrophils (NEU), lymphocytes (LYM), platelets (PLT), and hematocrit (HCT)

335   (Figure 3).

336   Compared to negative control, a significant increase in RBC, PLT concentration,

337   and HCT was detected at 3 dpi indicating elevated blood concentrations, and conversely,

338   at moribund states (14 dpi), the concentration decreased suggesting the occurrence of

339   hemorrhage, notably, RBC and HCT peaked at 3 dpi (8.76 and 46.7, respectively) and

340   PLT peaked at 7 dpi (1774) (Figure 3B, E and F). Meanwhile, a sharp decrease in the

341   concentration of WBC, NEU, and LYM was detected during the period of high viremia

342   (3 dpi), suggesting a possible inflammatory response of the organism, which peaked at

343   7 dpi as the virus was cleared from the bloodstream (13.07, 7.8 and 2.7, respectively)

344   (Figure 3A, C and D). None of the above assays were statistically different from

345   uninfected mice at moribund states.

346   In summary, hematological results indicated that DENV-I infected mice were

347   hemorrhagic and hemoconcentrated, but thrombocytopenia (which is clinically present
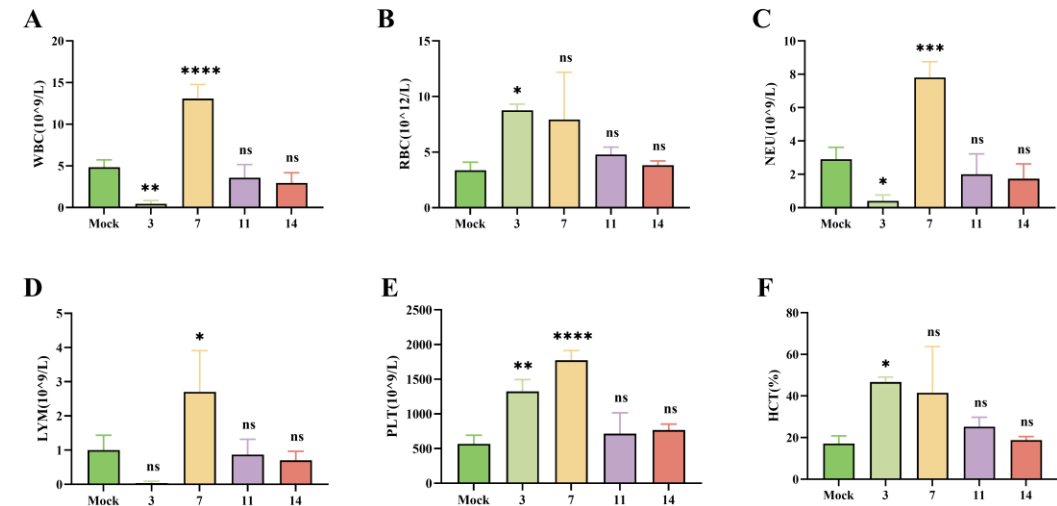
348   in 80% of patients) was not detected.

349

350   **Figure 3**. Hematology in DENV-I infected mice. AGB6 mice were IP. with 2.5 LD_{50} of

351   DENV-I. At the indicated time points. 3 mice per group per time point were bled and

352   euthanized. **(A)** Blood samples were processed to determine white blood cells (WBC),

353   **(B)** red blood cells (RBC), **(C)** neutrophils (NEU), **(D)** lymphocytes (LYM), **(E)**

354   platelets (PLT), **(F)** hematocrit (HCT) counts. Uninfected mice were used as controls.

355   WBC, NEU, LYM, and PLT counts are given in 10^9 cells/L, RBC counts in 10^{12} cells/L,

356   and HCT in percentage (%). Data are expressed as the mean±SD of individual

357   measurements. Ordinary one-way ANOVA test. *, $p < 0.05$; **, $p < 0.01$; ***, $p < 0.001$;

358   ****, $p < 0.0001$; ns, no significance.

359

360   ***DENV-I can be isolated from the brain tissue of infected AGB6 mice***

361   The mice were euthanized and the brain tissue was ground in PBS buffer and the

362   supernatant was taken for virus detection (Figure 4A). The supernatant was accessed

363   into Vero cells, and the indirect immunofluorescence assay could observe the same

364   fluorescence (Figure 4B) as the positive control (viral group), and the negative control

365   had no fluorescence. Then brain tissue virus isolates were serially passaged on C6/36

366   cells three times. Viral RNA copy numbers and cytopathic effects were evaluated at

367   each passage. The results showed that DENV-I isolates from the brain tissue could

368   induce cytopathic effects (CPE) in C6/36 cells within 7 days after inoculation

369   (Supplementary Table S2) and effectively replicated resulting in high viral RNA loads
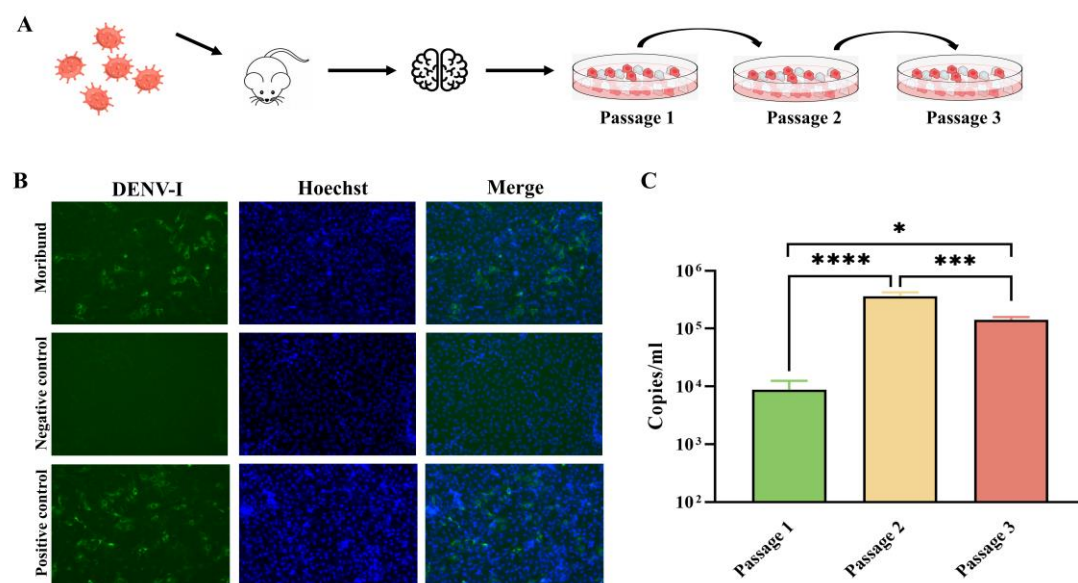
370   (up to 10^5 copies/ml) (Figure 4C).

371

372   **Figure 4**. Isolation of DENV-I from C6/36 and Vero cells. **(A)** Experimental scheme.

373   5-6 weeks old AGB6 mice were infected with 2.5 LD_{50} of DENV-I by IP.. The brain

374 tissues were harvested at moribund states. Isolates were passage-cultured for three
375 generations. **(B)** Indirect immunofluorescence assay for virus detection (green
376 fluorescent). **(C)** DENV-I was isolated from C6/36 cells and cultured for three passages;
377 viral loads were evaluated by RT-PCR. Ordinary one-way ANOVA test. *, $p < 0.05$;
378 ***, $p < 0.001$; ****, $p < 0.0001$.

379

380 ***RNA sequencing and differentially expressed genes in DENV-I infected AGB6 mice***
381 ***brain***

382   RNA-Seq analysis was performed using Illumina technology to compare the
383 differences in gene expression in brain tissues of infected and healthy control mice. The
384 samples obtained all provided complete and reasonable coverage of the different gene
385 structures and regions of the mouse reference genome, and the high and low gene
386 expression levels in each sample were calculated using the FPKM method
387 (Supplementary Figure S5 and Supplementary Table S3). Both inter-sample correlation
388 and principal component analysis (PCA) showed that there were significant differences
389 in gene expression between the two groups, which could be used for subsequent
390 analysis (Supplementary Fig. S6).

391   Subsequently, differentially expressed transcripts were screened based on the
392 criteria of log2 (fold change) $\geq |\pm 1|$ and adj. p-value $< = 0.05$. A total of 1,395 genes
393 were significantly differentially expressed in the brain in dengue virus infection model
394 mice: 1,301 upregulated and 94 downregulated genes (Supplementary figure S7A). The
395 differentially expressed genes between the two samples were characterized by
396 heatmaps and volcano plots (Supplementary figure S7B, C and Supplementary Table
397 S4).

398

399 ***Functional annotation of transcriptional changes***

400   To analyze the function of differentially expressed genes (DEGs), KEGG and GO
401 pathway enrichment analyses of the DEGs were performed using Cluster Profile
402 software, with p-adj less than 0.05 as the threshold for significant enrichment (Figure
403 5A, B).

404   We then performed the KEGG pathway enrichment analysis separately for up- and
405 down-regulated mRNA-related target genes. We found that up-regulated genes (1301
406 genes) were enriched for 76 significant pathways, in contrast, down-regulated genes
407 (94 genes) were enriched none pathway (Figure 5C and Supplementary Table S5).

408   Among them, the genes involved in Cytokine-cytokine receptor interaction, NF-kappa

409   B signaling pathway, Natural killer cell mediated cytotoxicity, Th17 cell differentiation,

410   the TNF signaling pathway and complement and coagulation cascades are activated

411   after DENV infection, which involves the expression of inflammatory cytokines and

412   the regulation of vascular permeability in the body, and these pathways have a closely

413   related to the pathogenesis of dengue virus infection.

414   GO enrichment can be categorized into three parts: biological process, cellular

415   composition, and molecular function (Figure 5D) and Supplementary Table S6). In the

416   gene ontology, the differential genes were found to be mainly involved in the processes

417   of immune system defense response, T cell and leukocyte activation, and cytokine-

418   cytokine interactions when compared with the control mouse brain tissues. Taken

419   together, the data showed that DENV infection induces a wide range of gene expression

420   changes, some of which were involved in viral infection and others in the host's
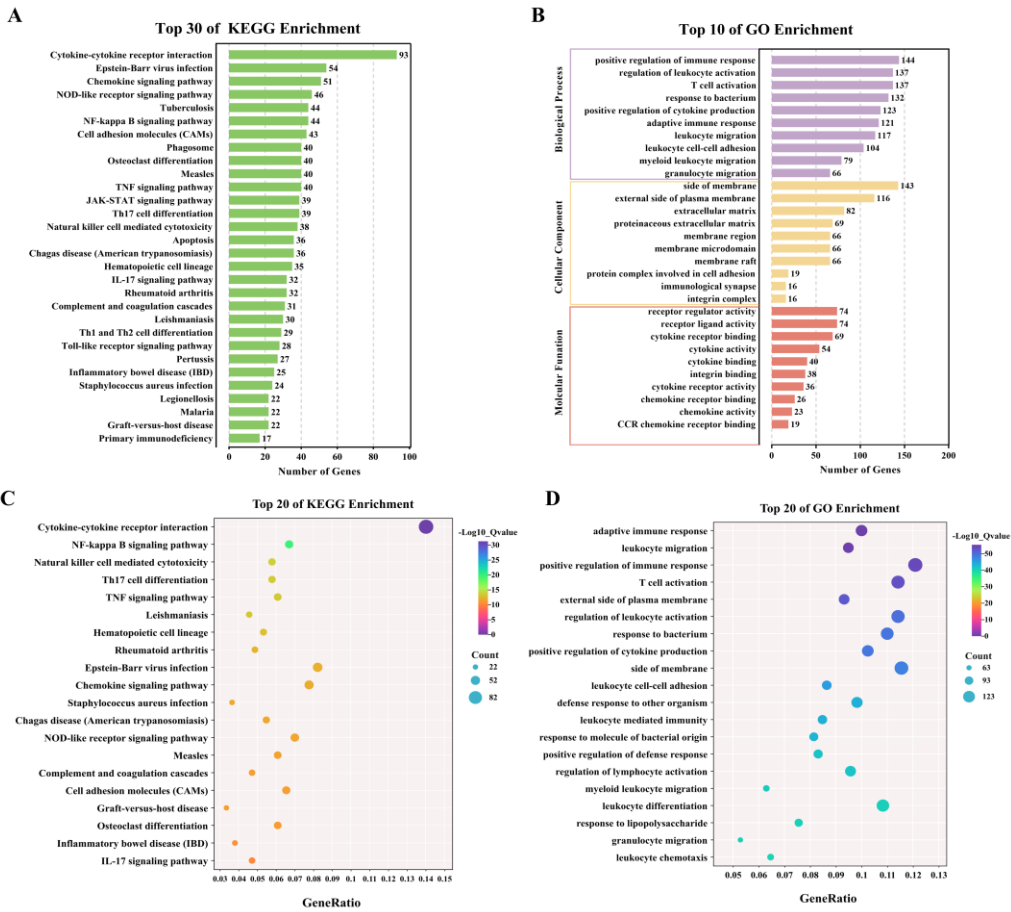
421   inflammatory and immune response.

422

423   **Figure 5**. Functional Annotation of Transcriptional Changes. **(A)** KEGG enrichment

424   analysis. **(B)** GO enrichment analysis was performed on the DEGs to describe their

425 functions. **(C)** KEGG enrichment of gene targets of all the up-regulated mRNA. **(D)**

426 GO enrichment of gene targets of all the up-regulated mRNA.

427

428 ***Protein interaction network analyses and preliminary identification of brain hub***

429 ***genes in DENV-I infected AGB6 mice***

430   We screened the DisGeNET and Genecard databases for genes associated with

431 severe dengue fever and dengue shock syndrome (Supplementary Table S7 and

432 Supplementary Table S8). After the removal of duplicated genes, 151 genes associated

433 with severe dengue were identified by comparison with those significantly upregulated

434 in this study. These genes were used for PPI analysis in the STRING database and

435 Cytoscape software was used for data visualization and analysis (Figure 6A and

436 Supplementary Table S9). We then performed tissue enrichment analysis

437 (Supplementary Table S10). We used the MCODE plugin in Cytoscape to cluster the

438 genes obtained from the screen (Figure 6B, C, and D) and Supplementary Table S11),

439 which mainly included cytokines that play essential roles in the immune system, such

440 as the Toll receptor family, chemokines, interleukins, interferons, and tumor necrosis

441 factors. The Cytohubba insert was selected to screen for Hubba genes, the first five of

442 which are TNF, IL-6, IL-1β, IFN-γ, and TLR4, which play essential roles in virus

443 recognition and innate immunity.

444   In order to clarify the expression of pro-inflammatory cytokines in brain tissues

445 after viral infection, RT-PCR and ELISA were utilized for analysis, respectively. First,

446 RT-PCR was utilized to identify these genes at the mRNA level, and the results showed

447 that viral infection resulted in significant upregulation of these four genes, with IL-6,

448 IL-1β and IFN-γ being the most significant (Figure 6E). Subsequently, the major

449 chemokines (CCL2, CCL3, CCL4, and CCL5) of the CCL family members, who are

450 also the major inflammatory chemokines in the cytokine storm, were assayed at the

451 mRNA level (Supplementary figure S8). Finally, the changes in the protein levels of

452 inflammatory factors in the brain tissue grinding fluid were analyzed, and the results

453 showed that the levels of IFN-γ and IL-6 proteins in the viral group were significantly

454 increased compared with those in the blank control group, whereas IL-1β and TNF-α

455 did not differ from those in the control group (Figure 6F). In conclusion, we surmise

456 that IL-6 and IFN-γ may be the key factors in dengue virus-induced neurological
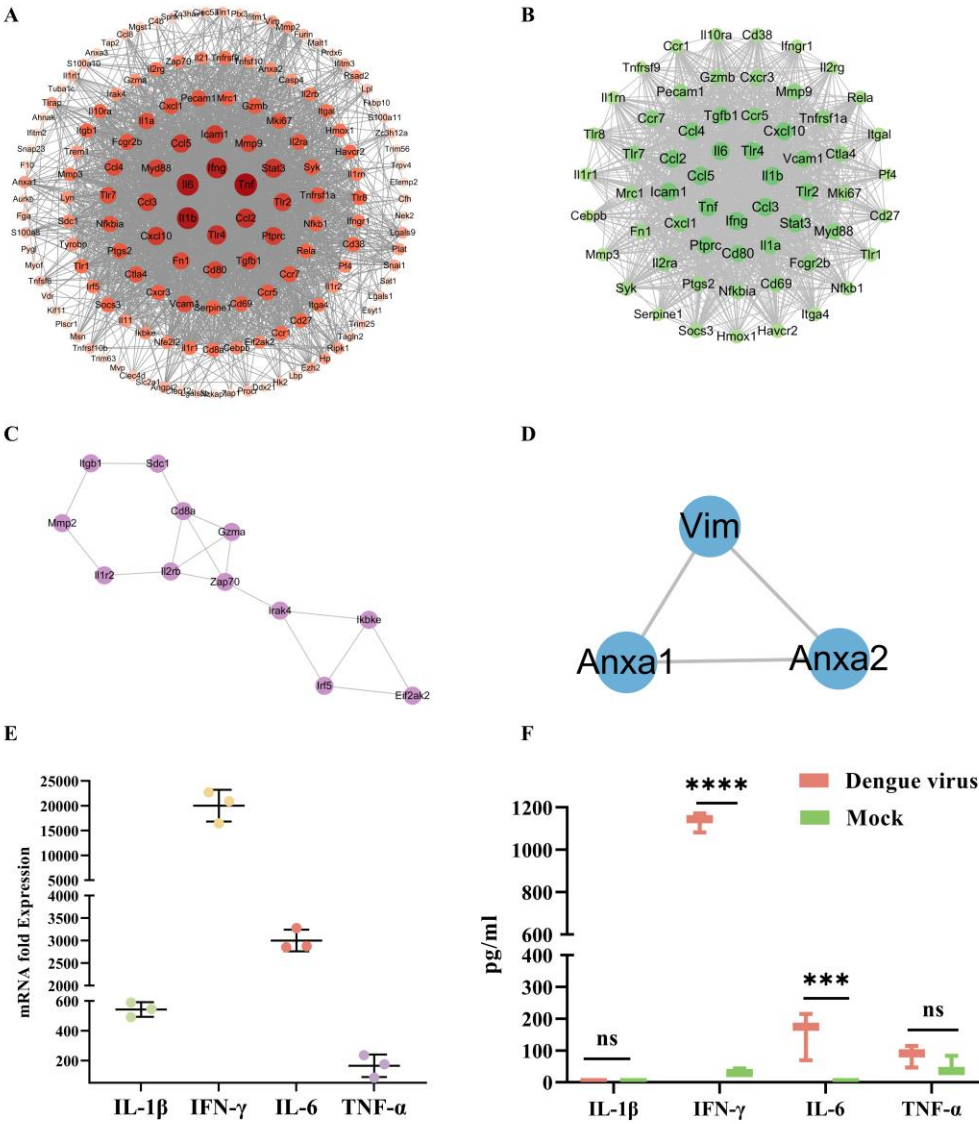
457 manifestations.

Figure 6. Screening for genes associated with DENV-I infection. **(A)** Network topology analysis and protein-protein interaction (PPI) networks of 151 differentially expressed genes between DENV-infected mice and controls. **(B-D)** The top three clusters that were significant from the PPI network. **(E)** Expression of pro-inflammatory cytokines in brain tissue after dengue virus infection (mRNA level). **(F)** Expression of pro-inflammatory factors in brain tissue (protein level). 2way ANOVA test. ***, $p < 0.001$; ****, $p < 0.0001$.

Discussion

Dengue virus infection is one of the significant public health problems globally,

469   especially in the tropical regions of the world, which account for 75 percent of dengue

470   cases. Although the majority of dengue virus infections are mild or asymptomatic, about

471   5 percent of cases progress to severe disease, mainly attributable to sequential infections

472   with different dengue virus serotypes[22]. For several years, the neurological

473   manifestations of dengue virus infection have become increasingly familiar and

474   understood and may be fatal if not treated promptly.

475   In 2009, the World Health Organization (WHO) issued new dengue guidelines and

476   a new classification that includes a definition of central nervous system involvement in

477   severe disease[23]. Currently, there are no mouse models that can be used to study

478   dengue virus-induced central nervous system (CNS) damage. AGB6 mice are type I

479   and type II interferon signaling pathway-deficient mice that have been used to study

480   dengue virus transmission[1]. In this study, AGB6 mice were selected as the

481   experimental animals, and intraperitoneal injection was used to establish a central

482   nervous system infection model. The results of the experimental study revealed a dose-

483   dependent dengue virus infection and infection of mice with a high dose (10^8 TCID$_{50}$)

484   induced an acute lethal dengue virus infection, a viral response consistent with the study

485   of Grace et al[18]. In contrast, infection of AGB6 mice with a low dose of the virus

486   resulted in a transient asymptomatic systemic viral infection, followed by the death of

487   the animal a few days after virus clearance, similar to the disease kinetics described in

488   human[24]. Meanwhile, at 10 dpi, mice show varying degrees of observable clinical

489   signs, including reversed coat, reduced activity, and weight loss. At 14 dpi, the

490   moribund states, the mice deteriorate and exhibit reduced locomotion and severe

491   manifestations of paralysis (hind limbs or unilateral hind limbs), which may lead to

492   reduced water intake and dehydration in the animals, resulting in dramatic weight loss

493   and ultimately death. The earliest studies in which mouse-adapted strains of DENV

494   virus were injected into mice[25], which developed neurologic symptoms, were once

495   thought to be unrelated to human clinical manifestations; however, the number of

496   reports of neurologic symptoms of dengue infections is increasing[26]. AG129 mice

497   infected intraperitoneally with DENV at a titer of 10^6 PFU similarly exhibited

498   neurologic abnormalities[27]. Intranasal inoculation of DENV-II at a titer of 2.4×10^5

499   PFU in adult A6 mice resulted in systemic infection and neurologic signs[19]. The

500   mouse-adapted strain DENV-II (D2S10) with a titer of 10^7 PFU was infected via

501   intraperitoneal infection of AG129 mice in a previous study without neurological

502   symptoms (paralysis), but the presence of virus was detected in neuronal tissue[28, 29].

503 The strains used in the above studies were mouse-adapted strains, and it is not possible
504 to determine whether or not the virus mutated in the mice to cause neurologic symptoms.
505 None of the previous studies had dengue virus infection of the nervous system as a
506 research objective, and unlike the previous studies, the strain of dengue virus used in
507 this study was isolated from human serum (not a mouse-adapted strain), and a
508 significant effect of high or low dosage and the duration of infection on the invasion
509 and pathogenicity of the virus was found by observing the severity of the pathological
510 changes in the brain tissues after the virus infection. The mouse infection model
511 established in this study can be used to study the pathogenicity of dengue virus on the
512 central nervous system and can be used for subsequent experimental studies.

513 Here, mice were infected with the virus by intraperitoneal injection, and as the
514 number of days of infection increased, the amount of virus in the brain gradually
515 increased, reaching a peak at moribund states. Expression of viral E protein could be
516 detected in brain tissue after 7 dpi. Extensive pathological damage was observed in both
517 the hippocampal region and the cerebral cortex of mouse brain tissue. Notably, the brain
518 tissue grinding supernatant can cause the cells to show CPE phenomenon. Instead, mild
519 damage was seen in the liver, spleen, and lungs, with NS3 antibody staining showing
520 weak positivity. Presumably, the brain is the primary target of this strain and may follow
521 a different mechanism of infection, further strengthening the evidence that dengue
522 viruses infect the central nervous system. It has been shown that dengue virus causes
523 widespread neurological involvement (e.g., transient muscle dysfunction, encephalitis),
524 with multiple disease manifestations reflecting one or more of the following causative
525 factors: metabolic disorders, autoimmune or excessive immune response, and direct
526 viral invasion[30]. Encephalitis is an inflammation of the brain parenchyma, usually
527 caused by viral infection. Direct viral invasion of the central nervous system, possibly
528 as a result of blood-brain barrier disruption, is the proposed pathogenesis of neurologic
529 involvement. In addition, autoimmune reactions and metabolic disorders have been
530 shown to further worsen neurologic deterioration[31, 32]. In our study, we found that
531 the brain tissue showed extensive pathological damage, with a large number of
532 inflammatory cells contained within dilated cerebral blood vessels, manifesting viral
533 encephalitis, and hematological tests revealed a mild elevation of leukocytes at 7 dpi.
534 Furthermore, previous studies illustrate vascular leakage as a hallmark of
535 DHF/DSS[33], leading to hemoconcentration and bleeding manifestations. Similarly,
536 an elevated erythrocyte specific volume at 3 dpi followed by a decrease at moribund

states (14 dpi) was detected in the present study. Notably, no hemorrhage was observed in pathological sections of brain tissue only vasodilatation was observed, whereas hemorrhage was observed in the liver of acutely dead mice. It was hypothesized that the strain isolated from patient sera are hypothesized to cause dengue hemorrhagic fever and encephalitis in mice, and the severity of the disease is closely related to the dose of infestation.

Hematology has been shown to be associated with dengue-associated diseases and has been used initially as a diagnostic and prognostic marker[34]. It has been shown that leukopenia often results in plasma leakage, which subsequently causes changes in capillary permeability and a massive release of cytokines or chemical mediators[35]. As large numbers of T cells are activated, a storm of cytokines is produced and acts on the vascular endothelium, which in turn manifests itself in hemorrhage, shock, and encephalopathy[36-38]. The possible mechanisms by which the virus causes the nervous system are passive transfer of CNS hemorrhage, plasma leakage or blood-brain barrier damage and infected monocyte/macrophage infiltration[30]. In this study, we found a significant decrease in leukocytes and a significant increase in erythrocyte and platelet concentrations in mice at the early stage of infection, and hematological indices suggesting an inflammatory response accompanied by hemorrhage. Infiltration of inflammatory cells is also seen in histopathologic sections of the brain. Previous studies have ruled out the possibility that lack of IFN-γ signaling due to mice impairs the thrombocytopenia mechanism[39], which required further study.

Based on transcriptomic analysis, among the significantly up-regulated genes, the major host pathways disrupted by dengue virus infection include cytokine-cytokine receptor interactions, the NF-kappa B signaling pathway, the TNF signaling pathway and complement and coagulation cascades which are thought to be involved in the pathogenesis of dengue fever closely related to the pathogenesis of dengue virus, and it is hypothesized that these factors are involved in brain tissue damage in mice. Recent studies have shown that cytokine overproduction in dengue virus infection leads to immune-mediated endothelial damage, which results in many CNS manifestations[13]. Cytokines such as tumor necrosis factor-α (TNF-α), which is usually elevated during the critical stages of dengue, may be essential cytokines in causing the disease[13]. DENV infection induces innate immunity in the host and promotes the production of pro-inflammatory factors and chemokines by immune cells, which further disrupts the blood-brain barrier (BBB) and subsequently facilitates the entry of other immune

571 mediators into the brain, leading to neuroinflammation[40-42]. Similarly, it has been

572 shown that NS1 antigen circulates in the bloodstream as a secreted glycoprotein that

573 promotes cytokine release[43]. Natural killer cells are involved in the pathogenesis of

574 neurological manifestations and activate T-helper (Th) cells, which differentiate into

575 Th17 and Th9 cells and promote the release of pro-inflammatory cytokines into the

576 brain to cause neuroinflammation (e.g., interferon-gamma, interleukin IL-12, IL-4, and

577 TGF-β)[44].

578 In our study, brain damage in DENV I-infected mice identified by RNA-Seq was

579 strongly associated with the release of inflammatory cytokines. IFN-β is a type I IFN

580 and an immunoregulatory cytokine that participates in innate antiviral immune defense

581 and regulates neuroinflammation[45, 46]. Recent studies have shown that blockage of

582 the IFN I pathway leads to mitochondrial dysfunction in the brain, resulting in neuronal

583 death[47]. In addition, platelets may further contribute to endothelial dysfunction

584 through the production of interleukin 1β (IL-1β) and other inflammatory cytokines by

585 monocytes, thereby causing neuroinflammation. It has been shown that DENV is highly

586 sensitive to the antiviral effects of type I and II interferons (IFN)[18], and that type I

587 and II IFNs control replication and dissemination of many viruses, including other

588 flaviviruses[48-50]. Pretreatment of human cells with alpha/bate IFN (IFN-α/β) and

589 IFN-γ)in a previous study protected them from DENV infection[51]. IFN-α/β receptor-

590 mediated effects limit initial DENV replication at peripheral sites and control viral

591 spread to the CNS, whereas IFN-γ receptor-mediated responses appear to play a role in

592 the later stages of DEN disease by limiting viral replication in the periphery and

593 removing virus from the CNS[52]. The AGB6 mice used in this study, which are type I

594 and type II IFN receptor-deficient mice, were used to model the infection, and the viral

595 load in the brain increased with the duration of infection after infection, and these

596 results are in agreement with the published report in which the DENV-II strain (PL046),

597 which has a titer of 10^8 PFU, was injected into AG129 mice, and paralytic symptoms

598 were observed, and the virus presence was detected in the nervous system[52].

599 Furthermore, from the data we obtained, it was found that the massive release of

600 cytokines plays an important role in the infection of the CNS by DENV. The study

601 found that the induction of cyclooxygenase-2 (PTGS2/COX2) by this cytokine in the

602 central nervous system (CNS) is found to contribute to inflammatory pain

603 hypersensitivity[47]. Equally important, IL-6, VCAM1, and ICAM1 are markers of

604 endothelial activation, in which IL-6 triggers local inflammation by promoting

leukocyte recruitment, and elevated VCAM1 and ICAM1 similarly increase endothelial cell permeability and promote the entry of cytokines in large quantities to elicit an inflammatory response[53-55].

Among the hub genes, TNF, IL-6, IL-1β, IFN-γ, and TLR4 are primarily associated with cytokine-cytokine receptor interactions. DENV infection prompts endothelial cells to release IL-6, CXCL10, and CXCL11, which increase the inflammatory response and vascular permeability, leading to plasma leakage in vivo[36]. The cytokines produced by T-cells, in addition to their role in viral clearance, promote inflammation and increase vascular permeability, which can lead to more severe disease. T-cell activation and cytokine production are observed during DHF in primary and secondary dengue virus infections [56, 57]. In severe dengue cases, a cascade of immune responses mediated by immune effectors increases the severity of the disease. Similar immune responses have been found in studies of other flaviviral infections of the nervous system, and blood-brain barrier damage induced by JEV infection was associated with increased secretion of inflammatory cytokines such as IL-1β, IL-6, and TNF-α[58]. ZIKV caused microcephaly and brain damage, and high levels of IL-1β and TNF-α were detected in the brain[59]. In order to clarify whether dengue virus-induced neurological infections follow the same mechanism of infection. In this study, high expression of IL-6, IL-1β, and IFN-γ at the mRNA level was detected by RT-PCR in brain tissues. Subsequently, the expression of inflammatory factor proteins in brain tissue was analyzed, and IFN-γ and IL-6 protein levels were significantly elevated compared to controls. It has been shown that IFN-γ and IL-6 directly affect the permeability of endothelial cells and increase the inflammatory response of the organism by inducing leukocyte recruitment, local inflammation, and damage to endothelial cells[54]. Further evidence that abnormal cytokine expression causes damage to the central nervous system.

In conclusion, the present study demonstrated that DENV can cause acute or chronic infection in AGB6 mice by intraperitoneal injection, which leads to neurological symptoms, high viral loads and significant pathological damage observed in brain tissues with clinical manifestations of paralysis. In addition, the potential mechanisms of CNS infection were initially explored by transcriptome sequencing. DENV infection in mice resulted in significant differences in the expression of a large number of genes in multiple signaling pathways in the host. Most of these differential genes (TNF, IL-6, IL-1β, IFN-γ, RELA, TLR4, VCAM1, and ICAM1) were associated

639   with host viral defense, further demonstrating the existence of antiviral immunity in the

640   CNS after DENV infection.

641

Supporting information

S1. Antibody titers in DENV-I-infected mice. (A) Specific anti-IgG titers were determined for each serum (1:51200). **(B)** Specific anti-IgM titers were determined for each serum (1:12800).

S2. DENV-I infection via the intraperitoneal route in C57BL/6 and BALB/c mice. (A) Body weight was monitored daily. Results are expressed as the [mean ± SD] of body weight loss in percentage compared to initial body weight. The mice showed no disease manifestations and continued to gain weight after infection. **(B)** Blood samples were harvested and viremia was evaluated (each time point, n=3). Low viral load and mild viremia were detected in the blood. **(C)** The organs of the challenged C57BL/6 mice were harvested, and the virus titer was evaluated using RT-PCR (each time point, n=3). **(D)** The organs of the challenged BALB/c were harvested, and the virus titer was evaluated using RT-PCR (each time point, n=3). Viral loads were low in each tissue organ. The dotted black line indicates the limits of detection.

S3. Tissue tropism and kinetic of virus replication in DENV-I infected mice. (A) The organs (heart, liver, spleen, lung, kidney, brain, jejunum, ileum, cecum, colon, rectum) of the challenged mice were harvested, and the viral load was evaluated. **(B)** DENV viral protein expression in mouse tissue was collected at 3, 7, 11, and 14 dpi via immunoblotting with an anti-E/NS1 antibody. **(C)** Representative H&E-stained tissue sections from the spleen, liver, and lung of AGB6 mice IP. infected with 2.52 LD_{50} of DENV-I. Animals were euthanized in moribund states. Sections were viewed under a light microscope at 200 × magnifications. **(D)** Immunohistochemical staining of tissue sections from the DENV-I infected mice with an anti-NS3 antibody.

S4. Histopathological study on Intestine, kidney, and heart. No noticeable histopathological changes were observed in these organs.

S5. (A) The number of raw reads and clean reads. (B) Quality control of clean data by $FastQC_{30}$. **(C)** The mapping rate and distribution of mapping reads to the reference genome.

S6. Gene expression statistics of RNA-Seq. **(A)** Boxplot of FPKM values for each independent sample. The box-and-whisker plot shows the dispersion degree of the data distribution. The horizontal axis shows the sample name, and the vertical axis shows the $\log_{10}(FPKM+1)$ values. **(B)** Plot of correlation coefficients between sequencing samples. The horizontal axis shows the sample name, the right vertical axis shows the corresponding sample name, and the color represents the magnitude of the correlation

coefficient. **(C)** Principal component analysis (PCA) was performed using the quantitative results of gene expression to investigate the distribution of samples.

S7. Identification of differentially expressed genes. (A) Statistical bar graph of differentially expressed genes. **(B)** Heatmap of differentially expressed genes. Unsupervised hierarchical clustering of differentially expressed genes. Samples from the two independent groups were assigned to the same cluster through cluster analysis. **(C)** Volcano plot of all genes in the samples from the two groups. The red dots correspond to upregulated genes, the blue dots correspond to downregulated genes, and the grey dots correspond to genes without statistically significant differences in expression.

S8. Expression of pro-inflammatory chemokines in brain tissue after dengue virus infection (mRNA level).

References

1. Lin JJ, Chung PJ, Dai SS, Tsai WT, Lin YF, Kuo YP, et al. Aggressive organ penetration and high vector transmissibility of epidemic dengue virus-2 Cosmopolitan genotype in a transmission mouse model. PLoS Pathog. 2021;17(3):e1009480. Epub 2021/03/31. https://dx.doi.org/10.1371/journal.ppat.1009480. PubMed PMID: 33784371; PubMed Central PMCID: PMCPMC8034735.

2. Tremblay N, Freppel W, Sow AA, Chatel-Chaix L. The Interplay between Dengue Virus and the Human Innate Immune System: A Game of Hide and Seek. Vaccines (Basel). 2019;7(4). Epub 2019/10/30. https://dx.doi.org/10.3390/vaccines7040145. PubMed PMID: 31658677; PubMed Central PMCID: PMCPMC6963221.

3. Guzman MG, Halstead SB, Artsob H, Buchy P, Farrar J, Gubler DJ, et al. Dengue: a continuing global threat. Nat Rev Microbiol. 2010;8(12 Suppl):S7-16. Epub 2010/11/17.

713   https://dx.doi.org/10.1038/nrmicro2460. PubMed PMID: 21079655; PubMed Central PMCID:
714   PMCPMC4333201.
715   4.   Aguiar M, Anam V, Blyuss KB, Estadilla CDS, Guerrero BV, Knopoff D, et al. Mathematical
716   models for dengue fever epidemiology: A 10-year systematic review. Phys Life Rev. 2022;40:65–
717   92. Epub 2022/02/28.   https://dx.doi.org/10.1016/j.plrev.2022.02.001. PubMed PMID: 35219611;
718   PubMed Central PMCID: PMCPMC8845267.
719   5.   Messina JP, Brady OJ, Scott TW, Zou C, Pigott DM, Duda KA, et al. Global spread of dengue
720   virus types: mapping the 70 year history. Trends Microbiol. 2014;22(3):138–46. Epub 2014/01/29.
721   https://dx.doi.org/10.1016/j.tim.2013.12.011. PubMed PMID: 24468533; PubMed Central PMCID:
722   PMCPMC3946041.
723   6.   Weaver SC, Vasilakis N. Molecular evolution of dengue viruses: contributions of phylogenetics
724   to understanding the history and epidemiology of the preeminent arboviral disease. Infect Genet
725   Evol.   2009;9(4):523-40.   Epub   2009/05/23.   https://dx.doi.org/10.1016/j.meegid.2009.02.003.
726   PubMed PMID: 19460319; PubMed Central PMCID: PMCPMC3609037.
727   7.   Harris E, Videa E, Pérez L, Sandoval E, Téllez Y, Pérez ML, et al. Clinical, epidemiologic, and
728   virologic features of dengue in the 1998 epidemic in Nicaragua. Am J Trop Med Hyg. 2000;63(1–
729   2):5-11. Epub 2001/05/19. https://dx.doi.org/10.4269/ajtmh.2000.63.5. PubMed PMID: 11357995.
730   8.   Guzman MG, Harris E. Dengue. Lancet. 2015;385(9966):453–65. Epub 2014/09/19.
731   https://dx.doi.org/10.1016/s0140-6736(14)60572-9. PubMed PMID: 25230594.
732   9.   WHO. Dengue and severe dengue 2023. Available from: https://www.who.int/zh/news-
733   room/fact-sheets/detail/dengue-and-severe-dengue.
734   10. WHO. Dengue guidelines, for diagnosis, treatment, prevention and control 2009. Available
735   from: https://www.who.int/publications/i/item/9789241547871.
736   11. Wiwanitkit   S, Wiwanitkit   V.   Neurological   complications   in   dengue   infection.   Arq
737   Neuropsiquiatr.   2014;72(3):259.   Epub   2014/03/29.   https://dx.doi.org/10.1590/0004-
738   282x20130222. PubMed PMID: 24676449.
739   12. Guzman MG, Gubler DJ, Izquierdo A, Martinez E, Halstead SB. Dengue infection. Nat Rev Dis
740   Primers.   2016;2:16055.   Epub   2016/08/19.   https://dx.doi.org/10.1038/nrdp.2016.55.   PubMed
741   PMID: 27534439.
742   13. Trivedi S, Chakravarty A. Neurological Complications of Dengue Fever. Curr Neurol Neurosci
743   Rep.   2022;22(8):515-29.   Epub   2022/06/22.   https://dx.doi.org/10.1007/s11910-022-01213-7.
744   PubMed PMID: 35727463; PubMed Central PMCID: PMCPMC9210046.
745   14. Puccioni-Sohler M, Orsini M, Soares CN. Dengue: a new challenge for neurology. Neurol Int.
746   2012;4(3):e15.   Epub   2013/01/29.   https://dx.doi.org/10.4081/ni.2012.e15.   PubMed   PMID:
747   23355928; PubMed Central PMCID: PMCPMC3555217.
748   15. Pandey A, Verma R, Jain A, Prakash S, Garg RK, Malhotra HS, et al. Correlation of serotype-
749   specific strain in patients with dengue virus infection with neurological manifestations and its
750   outcome. Neurol Sci. 2022;43(3):1939–46. Epub 2021/08/03. https://dx.doi.org/10.1007/s10072-
751   021-05477-8. PubMed PMID: 34338929.
752   16. Gupta S, Jesrani G, Cheema YS, Kumar V, Garg A. Dengue Encephalitis: A Case Series on a
753   Rare   Presentation   of   Dengue   Fever.   Cureus.   2022;14(1):e21615.   Epub   2022/03/02.
754   https://dx.doi.org/10.7759/cureus.21615. PubMed PMID: 35228969; PubMed Central PMCID:
755   PMCPMC8873623.
756   17. Wollner CJ, Richner M, Hassert MA, Pinto AK, Brien JD, Richner JM. A Dengue Virus Serotype

757 1 mRNA-LNP Vaccine Elicits Protective Immune Responses. J Virol. 2021;95(12). Epub 2021/03/26.
758 https://dx.doi.org/10.1128/jvi.02482-20. PubMed PMID: 33762420; PubMed Central PMCID:
759 PMCPMC8315947.
760 18.   Tan GK, Ng JK, Trasti SL, Schul W, Yip G, Alonso S. A non mouse-adapted dengue virus strain
761 as a new model of severe dengue infection in AG129 mice. PLoS Negl Trop Dis. 2010;4(4):e672.
762 Epub 2010/05/04.   https://dx.doi.org/10.1371/journal.pntd.0000672. PubMed PMID: 20436920;
763 PubMed Central PMCID: PMCPMC2860513.
764 19.   Qiu M, Zhao L, Zhang J, Wang Y, Liu M, Hua D, et al. Effective Infection with Dengue Virus in
765 Experimental Neonate and Adult Mice through the Intranasal Route. Viruses. 2022;14(7). Epub
766 2022/07/28.   https://dx.doi.org/10.3390/v14071394. PubMed PMID: 35891375; PubMed Central
767 PMCID: PMCPMC9322762.
768 20.   Kim D, Langmead B, Salzberg SL. HISAT: a fast spliced aligner with low memory requirements.
769 Nat Methods. 2015;12(4):357-60. Epub 2015/03/10.   https://dx.doi.org/10.1038/nmeth.3317.
770 PubMed PMID: 25751142; PubMed Central PMCID: PMCPMC4655817.
771 21.   Roberts A, Trapnell C, Donaghey J, Rinn JL, Pachter L. Improving RNA-Seq expression
772 estimates by correcting for fragment bias. Genome Biol. 2011;12(3):R22. Epub 2011/03/18.
773 https://dx.doi.org/10.1186/gb-2011-12-3-r22. PubMed PMID: 21410973; PubMed Central
774 PMCID: PMCPMC3129672.
775 22.   Khanam A, Gutiérrez-Barbosa H, Lyke KE, Chua JV. Immune-Mediated Pathogenesis in
776 Dengue   Virus   Infection.   Viruses.   2022;14(11).   Epub   2022/11/25.
777 https://dx.doi.org/10.3390/v14112575. PubMed PMID: 36423184; PubMed Central PMCID:
778 PMCPMC9699586.
779 23.   WHO Guidelines Approved by the Guidelines Review Committee. Dengue: Guidelines for
780 Diagnosis, Treatment, Prevention and Control: New Edition. Geneva: World Health Organization
781 Copyright © 2009, World Health Organization.; 2009.
782 24.   Whitehead SS, Blaney JE, Durbin AP, Murphy BR. Prospects for a dengue virus vaccine. Nat
783 Rev Microbiol. 2007;5(7):518-28. Epub 2007/06/15.   https://dx.doi.org/10.1038/nrmicro1690.
784 PubMed PMID: 17558424.
785 25.   Sabin AB, Schlesinger RW. PRODUCTION OF IMMUNITY TO DENGUE WITH VIRUS MODIFIED
786 BY   PROPAGATION   IN   MICE.   Science.   1945;101(2634):640-2.   Epub   1945/06/22.
787 https://dx.doi.org/10.1126/science.101.2634.640. PubMed PMID: 17844088.
788 26.   Li GH, Ning ZJ, Liu YM, Li XH. Neurological Manifestations of Dengue Infection. Front Cell
789 Infect Microbiol. 2017;7:449. Epub 2017/11/10.   https://dx.doi.org/10.3389/fcimb.2017.00449.
790 PubMed PMID: 29119088; PubMed Central PMCID: PMCPMC5660970.
791 27.   Johnson AJ, Roehrig JT. New mouse model for dengue virus vaccine testing. J Virol.
792 1999;73(1):783-6. Epub 1998/12/16.   https://dx.doi.org/10.1128/jvi.73.1.783-786.1999. PubMed
793 PMID: 9847388; PubMed Central PMCID: PMCPMC103889.
794 28.   Shresta S, Sharar KL, Prigozhin DM, Beatty PR, Harris E. Murine model for dengue virus-
795 induced lethal disease with increased vascular permeability. J Virol. 2006;80(20):10208-17. Epub
796 2006/09/29. https://dx.doi.org/10.1128/jvi.00062-06. PubMed PMID: 17005698; PubMed Central
797 PMCID: PMCPMC1617308.
798 29.   Zellweger RM, Prestwood TR, Shresta S. Enhanced infection of liver sinusoidal endothelial
799 cells in a mouse model of antibody-induced severe dengue disease. Cell Host Microbe.
800 2010;7(2):128-39. Epub 2010/02/16.   https://dx.doi.org/10.1016/j.chom.2010.01.004. PubMed

801   PMID: 20153282; PubMed Central PMCID: PMCPMC2824513.

802   30.   Solbrig MV, Perng GC. Current neurological observations and complications of dengue virus

803   infection.   Curr   Neurol   Neurosci   Rep.   2015;15(6):29.   Epub   2015/04/17.

804   https://dx.doi.org/10.1007/s11910-015-0550-4. PubMed PMID: 25877545.

805   31.   Domingues RB, Kuster GW, Onuki-Castro FL, Souza VA, Levi JE, Pannuti CS. Involvement of

806   the central nervous system in patients with dengue virus infection. J Neurol Sci. 2008;267(1-2):36-

807   40. Epub 2007/10/26.   https://dx.doi.org/10.1016/j.jns.2007.09.040. PubMed PMID: 17959198.

808   32.   Basu A, Chaturvedi UC. Vascular endothelium: the battlefield of dengue viruses. FEMS

809   Immunol   Med   Microbiol.   2008;53(3):287-99.   Epub   2008/06/05.

810   https://dx.doi.org/10.1111/j.1574-695X.2008.00420.x. PubMed PMID: 18522648; PubMed Central

811   PMCID: PMCPMC7110366.

812   33.   Trung DT, Wills B. Systemic vascular leakage associated with dengue infections - the clinical

813   perspective.   Curr   Top   Microbiol   Immunol.   2010;338:57-66.   Epub   2009/10/06.

814   https://dx.doi.org/10.1007/978-3-642-02215-9_5. PubMed PMID: 19802578.

815   34.   Binh PT, Matheus S, Huong VT, Deparis X, Marechal V. Early clinical and biological features of

816   severe clinical manifestations of dengue in Vietnamese adults. J Clin Virol. 2009;45(4):276-80. Epub

817   2009/05/20.   https://dx.doi.org/10.1016/j.jcv.2009.04.004. PubMed PMID: 19451025.

818   35.   Green S, Rothman A. Immunopathological mechanisms in dengue and dengue hemorrhagic

819   fever.   Curr   Opin   Infect   Dis.   2006;19(5):429-36.   Epub   2006/08/31.

820   https://dx.doi.org/10.1097/01.qco.0000244047.31135.fa. PubMed PMID: 16940865.

821   36.   Kurane I. Dengue hemorrhagic fever with special emphasis on immunopathogenesis. Comp

822   Immunol   Microbiol   Infect   Dis.   2007;30(5-6):329-40.   Epub   2007/07/25.

823   https://dx.doi.org/10.1016/j.cimid.2007.05.010. PubMed PMID: 17645944.

824   37.   Ulrich H, Pillat MM, Tárnok A. Dengue Fever, COVID-19 (SARS-CoV-2), and Antibody-

825   Dependent Enhancement (ADE): A Perspective. Cytometry A. 2020;97(7):662-7. Epub 2020/06/09.

826   https://dx.doi.org/10.1002/cyto.a.24047.   PubMed   PMID: 32506725;   PubMed   Central   PMCID:

827   PMCPMC7300451.

828   38.   Harapan H, Ryan M, Yohan B, Abidin RS, Nainu F, Rakib A, et al. Covid-19 and dengue: Double

829   punches   for   dengue-endemic   countries   in   Asia.   Rev   Med   Virol.   2021;31(2):e2161.   Epub

830   2020/09/19.   https://dx.doi.org/10.1002/rmv.2161.   PubMed   PMID: 32946149;   PubMed   Central

831   PMCID: PMCPMC7536968.

832   39.   Williams KL, Zompi S, Beatty PR, Harris E. A mouse model for studying dengue virus

833   pathogenesis and immune response. Ann N Y Acad Sci. 2009;1171 Suppl 1:E12-23. Epub

834   2009/09/16.   https://dx.doi.org/10.1111/j.1749-6632.2009.05057.x. PubMed PMID: 19751398.

835   40.   Garcia M, Wehbe M, Lévêque N, Bodet C. Skin innate immune response to flaviviral infection.

836   Eur   Cytokine   Netw.   2017;28(2):41-51.   Epub   2017/08/26.

837   https://dx.doi.org/10.1684/ecn.2017.0394. PubMed PMID: 28840835.

838   41.   Loo YM, Gale M, Jr. Immune signaling by RIG-I-like receptors. Immunity. 2011;34(5):680-92.

839   Epub 2011/05/28.   https://dx.doi.org/10.1016/j.immuni.2011.05.003.   PubMed   PMID: 21616437;

840   PubMed Central PMCID: PMCPMC3177755.

841   42.   Akira S, Takeda K. Toll-like receptor signalling. Nat Rev Immunol. 2004;4(7):499-511. Epub

842   2004/07/02.   https://dx.doi.org/10.1038/nri1391. PubMed PMID: 15229469.

843   43.   Libraty DH, Young PR, Pickering D, Endy TP, Kalayanarooj S, Green S, et al. High circulating

844   levels of the dengue virus nonstructural protein NS1 early in dengue illness correlate with the

845 development of dengue hemorrhagic fever. J Infect Dis. 2002;186(8):1165-8. Epub 2002/10/02.

846 https://dx.doi.org/10.1086/343813. PubMed PMID: 12355369.

847 44. Salazar MI, Pérez-García M, Terreros-Tinoco M, Castro-Mussot ME, Diegopérez-Ramírez J,

848 Ramírez-Reyes AG, et al. Dengue virus type 2: protein binding and active replication in human

849 central nervous system cells. ScientificWorldJournal. 2013;2013:904067. Epub 2013/12/05.

850 https://dx.doi.org/10.1155/2013/904067. PubMed PMID: 24302878; PubMed Central PMCID:

851 PMCPMC3835358.

852 45. Teige I, Treschow A, Teige A, Mattsson R, Navikas V, Leanderson T, et al. IFN-beta gene

853 deletion leads to augmented and chronic demyelinating experimental autoimmune

854 encephalomyelitis. J Immunol. 2003;170(9):4776-84. Epub 2003/04/23.

855 https://dx.doi.org/10.4049/jimmunol.170.9.4776. PubMed PMID: 12707359.

856 46. Rothhammer V, Mascanfroni ID, Bunse L, Takenaka MC, Kenison JE, Mayo L, et al. Type I

857 interferons and microbial metabolites of tryptophan modulate astrocyte activity and central

858 nervous system inflammation via the aryl hydrocarbon receptor. Nat Med. 2016;22(6):586-97.

859 Epub 2016/05/10. https://dx.doi.org/10.1038/nm.4106. PubMed PMID: 27158906; PubMed

860 Central PMCID: PMCPMC4899206.

861 47. Magalhaes J, Tresse E, Ejlerskov P, Hu E, Liu Y, Marin A, et al. PIAS2-mediated blockade of

862 IFN-β signaling: a basis for sporadic Parkinson disease dementia. Mol Psychiatry.

863 2021;26(10):6083-99. Epub 2021/07/09. https://dx.doi.org/10.1038/s41380-021-01207-w.

864 PubMed PMID: 34234281; PubMed Central PMCID: PMCPMC8758491.

865 48. Aliota MT, Caine EA, Walker EC, Larkin KE, Camacho E, Osorio JE. Characterization of Lethal

866 Zika Virus Infection in AG129 Mice. PLoS Negl Trop Dis. 2016;10(4):e0004682. Epub 2016/04/20.

867 https://dx.doi.org/10.1371/journal.pntd.0004682. PubMed PMID: 27093158; PubMed Central

868 PMCID: PMCPMC4836712.

869 49. Keller BC, Fredericksen BL, Samuel MA, Mock RE, Mason PW, Diamond MS, et al. Resistance

870 to alpha/beta interferon is a determinant of West Nile virus replication fitness and virulence. J Virol.

871 2006;80(19):9424-34. Epub 2006/09/16. https://dx.doi.org/10.1128/jvi.00768-06. PubMed PMID:

872 16973548; PubMed Central PMCID: PMCPMC1617238.

873 50. Lobigs M, Müllbacher A, Wang Y, Pavy M, Lee E. Role of type I and type II interferon responses

874 in recovery from infection with an encephalitic flavivirus. J Gen Virol. 2003;84(Pt 3):567-72. Epub

875 2003/02/27. https://dx.doi.org/10.1099/vir.0.18654-0. PubMed PMID: 12604807.

876 51. Diamond MS, Roberts TG, Edgil D, Lu B, Ernst J, Harris E. Modulation of Dengue virus infection

877 in human cells by alpha, beta, and gamma interferons. J Virol. 2000;74(11):4957-66. Epub

878 2000/05/09. https://dx.doi.org/10.1128/jvi.74.11.4957-4966.2000. PubMed PMID: 10799569;

879 PubMed Central PMCID: PMCPMC110847.

880 52. Shresta S, Kyle JL, Snider HM, Basavapatna M, Beatty PR, Harris E. Interferon-dependent

881 immunity is essential for resistance to primary dengue virus infection in mice, whereas T- and B-

882 cell-dependent immunity are less critical. J Virol. 2004;78(6):2701-10. Epub 2004/03/03.

883 https://dx.doi.org/10.1128/jvi.78.6.2701-2710.2004. PubMed PMID: 14990690; PubMed Central

884 PMCID: PMCPMC353772.

885 53. John DV, Lin YS, Perng GC. Biomarkers of severe dengue disease - a review. J Biomed Sci.

886 2015;22:83. Epub 2015/10/16. https://dx.doi.org/10.1186/s12929-015-0191-6. PubMed PMID:

887 26462910; PubMed Central PMCID: PMCPMC4604634.

888 54. Neumann FJ, Ott I, Marx N, Luther T, Kenngott S, Gawaz M, et al. Effect of human recombinant

889 interleukin-6 and interleukin-8 on monocyte procoagulant activity. Arterioscler Thromb Vasc Biol.
890 1997;17(12):3399-405. Epub 1998/01/23. https://dx.doi.org/10.1161/01.atv.17.12.3399. PubMed
891 PMID: 9437185.

892 55. Vitoria WO, Thomé LS, Kanashiro-Galo L, Carvalho LV, Penny R, Santos WLC, et al.
893 Upregulation of intercellular adhesion molecule-1 and vascular cell adhesion molecule-1 in renal
894 tissue in severe dengue in humans: Effects on endothelial activation/dysfunction. Rev Soc Bras
895 Med Trop. 2019;52:e20180353. Epub 2019/11/30. https://dx.doi.org/10.1590/0037-8682-0353-
896 2018. PubMed PMID: 31778418.

897 56. Cruz Hernández SI, Puerta-Guardo HN, Flores Aguilar H, González Mateos S, López Martinez
898 I, Ortiz-Navarrete V, et al. Primary dengue virus infections induce differential cytokine production
899 in Mexican patients. Mem Inst Oswaldo Cruz. 2016;111(3):161-7. Epub 2016/03/24.
900 https://dx.doi.org/10.1590/0074-02760150359. PubMed PMID: 27008374; PubMed Central
901 PMCID: PMCPMC4804498.

902 57. Sierra B, Pérez AB, Alvarez M, García G, Vogt K, Aguirre E, et al. Variation in
903 inflammatory/regulatory cytokines in secondary, tertiary, and quaternary challenges with dengue
904 virus. Am J Trop Med Hyg. 2012;87(3):538-47. Epub 2012/07/18.
905 https://dx.doi.org/10.4269/ajtmh.2012.11-0531. PubMed PMID: 22802438; PubMed Central
906 PMCID: PMCPMC3435361.

907 58. Thounaojam MC, Kaushik DK, Kundu K, Basu A. MicroRNA-29b modulates Japanese
908 encephalitis virus-induced microglia activation by targeting tumor necrosis factor alpha-induced
909 protein   3.   J   Neurochem.   2014;129(1):143-54.   Epub   2013/11/19.
910 https://dx.doi.org/10.1111/jnc.12609. PubMed PMID: 24236890.

911 59. Shao Q, Herrlinger S, Yang SL, Lai F, Moore JM, Brindley MA, et al. Zika virus infection disrupts
912 neurovascular development and results in postnatal microcephaly with brain damage.
913 Development. 2016;143(22):4127-36. Epub 2016/11/02. https://dx.doi.org/10.1242/dev.143768.
914 PubMed PMID: 27729407; PubMed Central PMCID: PMCPMC5117220.

915